

Monte Carlo simulation of Nb $K\alpha$ secondary fluorescence in EPMA: comparison of PENELOPE simulations with experimental results

John H. Fournelle,^{1*} Sungtae Kim² and John H. Perepezko²

¹ Department of Geology and Geophysics, University of Wisconsin, 1215 W. Dayton St., Madison, WI 53706, USA

² Department of Material Science and Engineering, University of Wisconsin, Madison, WI 53706, USA

Received 19 January 2005; Revised 27 April 2005; Accepted 27 April 2005

Secondary fluorescence across phase boundaries is a difficult problem encountered in several electron probe microanalysis (EPMA) situations: diffusion couples; small phases enclosed in a larger phases; eutectic intergrowths; and thin films. In some cases, it is possible to construct nondiffused couples and to measure the amount of secondary fluorescence across the phase boundary, but in most cases this is difficult, time consuming, expensive, or impossible. It is thus desirable to model the secondary fluorescence by Monte Carlo methods. Here we compare the results of experimentally measured secondary fluorescence of Nb $K\alpha$ with results from the PENELOPE Monte Carlo program, and find that there is close correspondence. Copyright © 2005 John Wiley & Sons, Ltd.

KEYWORDS: EPMA; fluorescence; secondary fluorescence; EDS; WDS; Monte Carlo; PENELOPE

INTRODUCTION

Most researchers utilizing EDS (energy dispersive spectrometry) and WDS (wavelength dispersive spectrometry) measurements with scanning electron microscopes and electron microprobes are cognizant of the scattering of incident high voltage electrons within the specimen, resulting in an interaction volume or electron range of fractions to several micrometers in diameter/length. An unspoken assumption in EDS and WDS matrix corrections is that there are no different phases within 'striking distance' of the X rays generated. Less well appreciated is the ability of the X rays generated within the primary electron's interaction volume to travel long distances (tens to hundreds of micrometers, depending on several factors) and to interact with atoms far from the original electron target site. These X rays (both characteristic and continuum) have the ability to excite additional X rays, i.e. secondarily fluoresce, in materials different from the original material – and thus yield erroneous results.¹ This study examines that situation.

In 2003, we examined an annealed Nb–Pd–Hf–Al sample (Fig. 1) to determine if the Pd_3Hf and Pd_2HfAl phases had significant Nb solubility in them; the third phase present was Nb solid solution (ss). Another group had determined compositions using EDS analysis, measuring Nb $K\alpha$ with an accelerating voltage of 30 keV and found ~10 wt% Nb in both phases (Fig. 2; Table 1). The alternative Nb line, Nb $L\alpha$, is overlapped by several of the Pd L lines in EDS.

*Correspondence to: John H. Fournelle, Department of Geology and Geophysics, University of Wisconsin, 1215 W. Dayton St., Madison, WI 53706, USA. E-mail: johnf@geology.wisc.edu

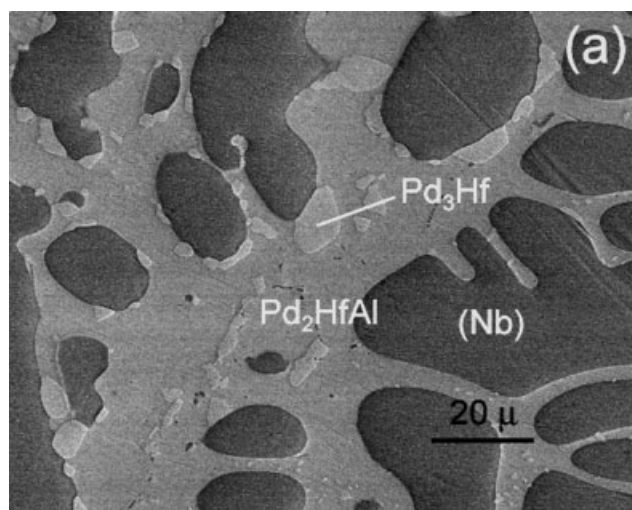


Figure 1. BSE image of annealed experimental sample.

At that time, we had EPMA WDS capability only to measure Nb $L\alpha$. Our 18-keV EPMA measurement showed little or no Nb (Table 1).

The textural relations – a eutectic assemblage with the problematic phases intergrown 10–30 μm (in x – y , presumably the same in z) from Nb ss – suggested secondary fluorescence as an explanation of the discrepancy between the Nb $K\alpha$ EDS and Nb $L\alpha$ WDS results. We decided to test this experimentally with a nondiffused couple of Nb pressed against Pd_2HfAl , and acquired an LIF220 crystal ($2d = 0.2848$ nm) that would permit WDS EPMA measurement of Nb $K\alpha$.

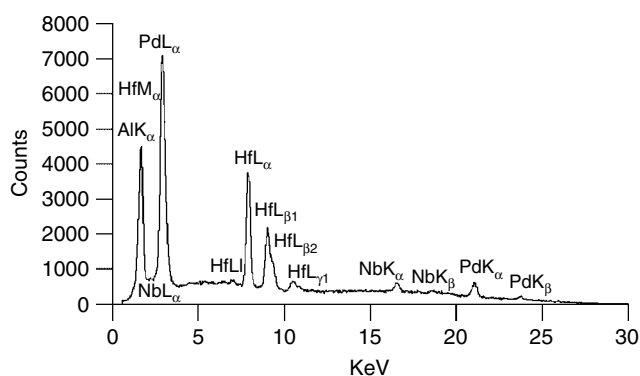


Figure 2. Actual EPMA EDS spectrum within Pd₂HfAl at 5 μm distance from boundary with Nb. Conditions: 30 keV; 37% deadtime; 200 s.

Table 1. Measurements from annealed experimental sample: original EDS data at 30 keV Nb K α plus WDS Nb L α at 18 keV

EDS, 30 keV, with Nb K α					
	Nb wt%	Pd wt%	Hf wt%	Al wt%	Sum
Nb ss	87.25	9.10	2.97	0.68	100
Pd ₂ HfAl	9.95	54.66	29.59	5.81	100
Pd ₃ Hf	10.10	58.96	30.94	0.00	100
WDS, 18 keV, with Nb L α					
	Nb wt%	Pd wt%	Hf wt%	Al wt%	Sum
Nb ss	91.32	8.85	2.90	0.63	103.69
Pd ₂ HfAl	0.48	59.07	33.98	5.71	99.25
Pd ₃ Hf	0.00	64.86	35.77	0.04	100.68

EXPERIMENTAL

WDS EPMA measurements were made with the UW-Madison Cameca SX51 electron microprobe, utilizing Probe for Windows-Enterprise software.² Samples were polished, not carbon coated, and the experimental phases far from the interface were used as the analytical standards. Matrix corrections were performed with Armstrong's³ phi-rho-z procedure (modified from Brown and Bastin).

WDS measurements of the experimental phases were made at 28 keV (60 nA) of Nb K α and L α (20 nA) of both Pd₃Hf and Pd₂HfAl at least 10 μm laterally from the nearest Nb ss phase. (The electron range in the Pd₂HfAl was 1.5–2 μm, determined with the CASINO⁴ program.) Concentrations evaluated from Nb L α X rays were essentially zero, but those evaluated from Nb K α ranged from 4 to 10 wt% Nb with analytical wt% totals greater than 100 by approximately that 'excess' Nb K α amount (Table 2). Peak and background count times for Nb K α were 40 s each (for Nb L α , 22 s). Gas flow detector ionization efficiency by Ar in the P10 gas for Nb K α is rather low, resulting in the detection limit being 1.5 wt%.

A nondiffused couple was created by squeezing polished Nb against polished Pd₂HfAl between stainless steel clamps, placed in epoxy and polished. WDS measurement at 28 keV of Nb K α and L α across the interface, from Nb to Pd₂HfAl,

Table 2. Measurements from annealed experimental sample: WDS at 28 keV Nb K α and L α

WDS, 28 keV, with Nb L α					
	Nb wt%	Pd wt%	Hf wt%	Al wt%	Sum
Nb ss	93.02	8.05	2.35	0.51	103.90
Pd ₂ HfAl	0.32	61.41	32.46	5.38	99.58
Pd ₃ Hf	0.04	67.60	34.41	0.03	102.10
WDS, 28 keV, with Nb K α (LIF220)					
	Nb wt%	Pd wt%	Hf wt%	Al wt%	Sum
Nb ss	87.39	8.02	2.35	0.52	98.28
Pd ₂ HfAl	5.15	62.99	32.50	5.36	105.99
Pd ₃ Hf	11.28	71.31	34.49	0.03	117.11

showed essentially no secondary fluorescence of the Nb L α , whereas there was clear evidence of secondary fluorescence for Nb K α , ranging from an apparent Nb content of 9 wt% at 3 μm, 4.5 wt% at 10 μm, to 1.5 wt% (the detection limit) at 28 μm from the interface (Fig. 3). This supports the hypothesis that Nb K α secondary fluorescence is very significant.

The ability to experimentally reproduce secondary fluorescence with a nondiffused couple is not readily possible in many situations. With the spread of powerful personal computers, Monte Carlo simulation of electron-specimen interactions is readily available. Secondary fluorescence across phase boundaries is not included in most models. Fortunately, photon transport in matter has been modeled with the Monte Carlo program PENELOPE,⁵ and has been shown to accurately reproduce secondary fluorescence.^{6,7} PENELOPE has the ability to model different accelerating voltages and position a detector at different take-off angles (here we used 40°). The original version of PENELOPE used to acquire data here had one annular detector (with the proper take-off angle), which although physically unrealistic, speeded up computation.

Our original PENELOPE simulations were run for 8–18 h each; an 807 MHz PC simulated 97 electron showers (individual electron trajectory histories) per second, whereas a 1.2 GHz iBook ran 136 showers per second. The time-limiting step was needed to acquire high quality (3 sigma precision) continuum (off-peak background) measurements on both sides of the Nb K α peak for subtraction prior to determination of the K-ratio (intensity of Nb K α in the unknown divided by its intensity in the standard). Figure 4 shows the simulated energy spectrum of the PENELOPE output for a 50-min run at 5 μm from the interface, away from the Nb ss side. The continuum shows an irregular nature, and requires 8–10 h to develop a higher precision.

We had the opportunity to utilize a more recent beta version (2005) that has significant modifications, including the elimination of the need to acquire off-peak background measurements, as the program intelligently tallies only characteristic X rays, with each generated X ray tagged to its generation mode. This speeds up computation. Another modification is the ability to position up to ten detectors of

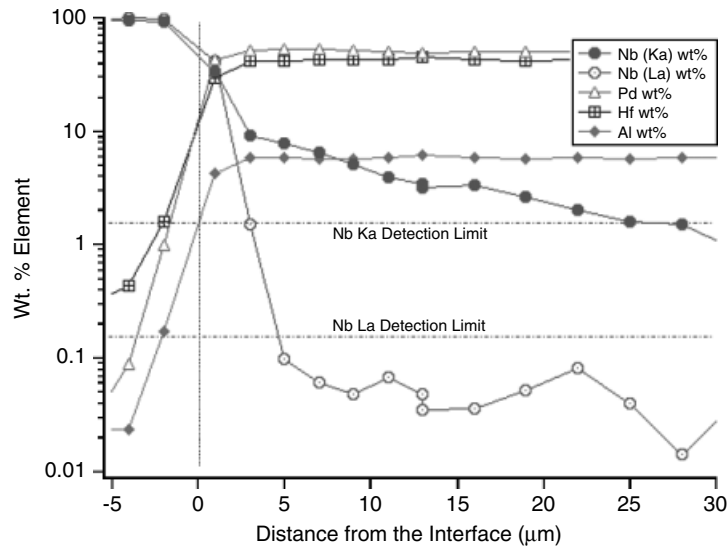


Figure 3. Plot of Nb, Pd, Hf and Al wt% values measured in a nondiffused couple (Nb to left, Pd₂HfAl to right) measured by WDS EPMA. Measurements for Nb are given for both Nb K α and Nb L α , with associated minimum detection levels. The apparent high level of Nb present when Nb K α is measured is a result of secondary fluorescence, both from Pd K α and K β and from the continuum above the Nb K edge at 18.986 keV.

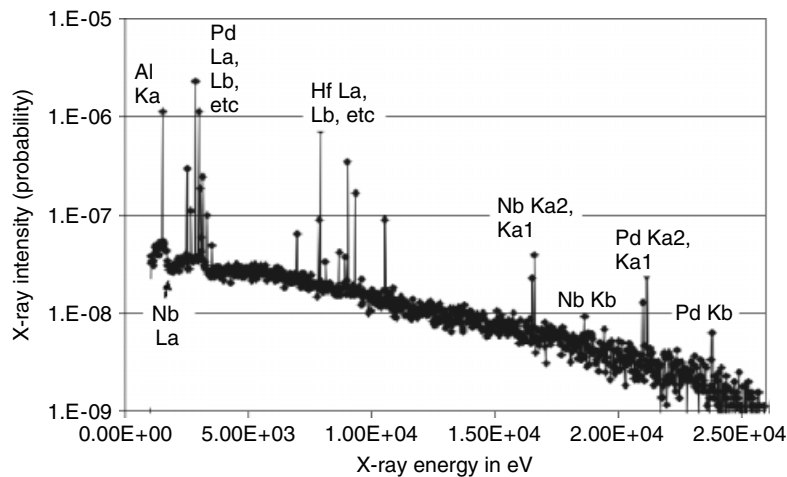


Figure 4. Penelope simulated energy spectrum; 50 min simulation time, original PENELOPE version with continuum saved and displayed. Simulation stops for each electron in shower when its energy reaches 1000 eV.

any take-off angle, azimuth, or acceptance window size. This will be discussed in the following text.

RESULTS AND DISCUSSION

We have modeled EPMA in the diffusion couple geometry with PENELOPE to validate its simulation of secondary fluorescence. The original simulations with PENELOPE generated K -ratios with a very similar curve as the experimental data but offset to somewhat higher values (e.g. 0.07 vs 0.04 seen experimentally at 10 μ m from the interface). Further investigation suggested that the geometry of the sample interface relative to the detector position might be significant, both in the actual EPMA experiment and in the PENELOPE simulation geometry.

The spectrometer with the LIF220 crystal was at the eleven o'clock position, and the original nondiffused couple was positioned nonorthogonally with it, the Nb-metal side

facing away from the spectrometer. This was different from the original PENELOPE geometry, with an annular detector above the specimen, where there would not be any preferential direction for detection of secondary fluoresced X rays.

With the PENELOPE beta 2005 version, we redefined the problem with a variety of smaller angular detectors at various azimuths to the Nb–Pd₂HfAl interface; many runs were made at one distance (20 μ m from the interface) to verify that the geometry actually made a difference. Figure 5 shows the results, which indicate that there is a significant difference dependent upon detector position relative to the materials, with >40% greater secondary fluorescence intensities if the Nb side faces the detector.

We reacquired the experimental EPMA data with the nondiffused couple mounted orthogonally to the detector (projected on the x – y plane of the stage) in two orientations:

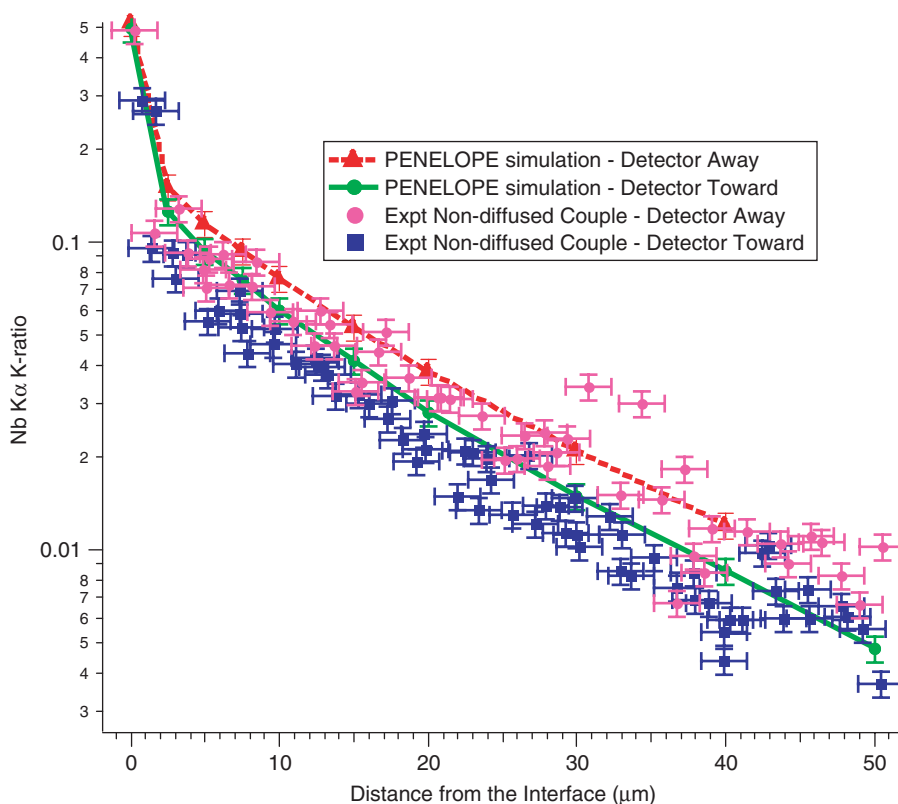


Plate 1. Plot of Nb K_{α} K-ratio versus distance: two PENELOPE simulations (open symbols, connected by lines) versus two sets of experimental data (closed symbols). Squares represent (lower) experimental K-ratios where the Nb side is facing away from the LIF220 detector; circles represent (higher) K-ratios where the Nb side is facing toward the detector. The dashed line with triangles represents the PENELOPE simulation of (higher) K-ratios where the Nb side faces the detector; solid line with open circles represents the PENELOPE simulation of (lower) K-ratios where Nb side faces away from detector. EPMA experimental data intensity error bars are 10% of value, which is appropriate in the 20–30 μm range; bars at $<20 \mu\text{m}$ should be smaller (\sim half), and those $>30 \mu\text{m}$ should be two to three times larger. The PENELOPE error bars are 10% of value, appropriate for $\geq 30 \mu\text{m}$, and should be smaller (\sim half) for $<30 \mu\text{m}$.

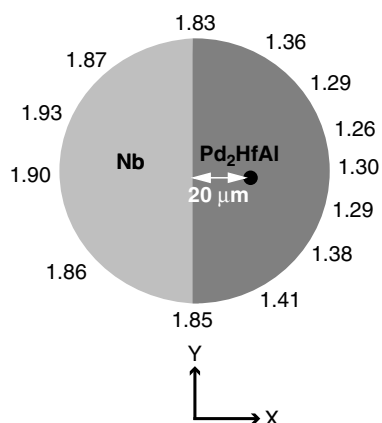


Figure 5. Results with PENELOPE beta 2005 version using detectors at different positions: secondary fluorescent Nb $K\alpha$ photons produced by 28 keV electrons impacting 20 μm to the right of the interface, away from the Nb. Results of multiple high precision simulations with smaller detectors situated at various azimuths to the sample are given. Values are Nb $K\alpha$ intensities as probabilities ($\times 10^{-8}$). Detectors that would have greatest probability of acquiring Nb $K\alpha$ and did not interact with Pd₂HfAl have 40% higher counts than detectors with greater probability of acquiring Nb $K\alpha$ that 'stumbled' back through Pd₂HfAl before being detected. Geometry of PENELOPE target is a 1 cm radius cylinder, divided in half into two materials as shown in the figure.

with the Nb-metal side facing toward the detector, and facing away from it.

The results showed that when the Nb side faced the detector, there were higher counts of secondarily fluoresced Nb $K\alpha$, and when the Nb side was 180° away, there were lower counts (Plate 1).

One factor responsible for this behavior is the differential absorption of the Nb $K\alpha$ X rays in the material through which they pass. The mass absorption coefficient of Nb $K\alpha$ by Nb is 20, whereas for Pd₂HfAl it is 57. It seems reasonable that there will be less absorption of the X rays when the Nb material is closer to the off-center detector, rather than the 180° opposite case. Further work is called for here in evaluating the actual paths of simulated secondary fluorescent photons in PENELOPE history files.

The results of the two PENELOPE geometries with detectors in opposite directions relative to the Nb metal are in good agreement with the experimental data gathered in two similar geometries. The 'detector toward Nb' simulation and experimental data are in near-perfect agreement, whereas the 'detector away from Nb' simulation appears to be consistently slightly higher than the experimental data. We are investigating the significance of this with the PENELOPE authors.

We have demonstrated both with experiment and with Monte Carlo simulation the existence of significant Nb $K\alpha$ secondary fluorescence. The magnitude of this stems from two aspects: (i) the system contains Pd, which when ionized to yield Pd $K\alpha$ X rays (21.18 keV) is optimally coupled in the pantheon of X-ray absorption energies to excite Nb (K edge at 18.99 keV) and (ii) analytical conditions consist of high

Table 3. Mass absorption coefficients⁸ (μ/ρ) for Nb $L\alpha$ and $K\alpha$ for each element in the samples

Mass absorption coefficients				
	Al	Nb	Pd	Hf
Nb $L\alpha$	1899	718	1068	3521
Nb $K\alpha$	6	20	28	100

accelerating voltage (28 or 30 keV), which both excite Pd $K\alpha$ (see before) and also produce continuum X rays greater than 19 keV which will also generate some secondary Nb $K\alpha$ X rays.

In all cases, Nb $L\alpha$ showed no secondary fluorescence beyond possibly a couple of micrometers from the phase boundary. Examination of the mass absorption coefficients for Nb $L\alpha$ versus Nb $K\alpha$ shows the magnitude of the difference, and why there is little probability that any Nb $L\alpha$ X rays will travel more than a few micrometers in a material containing Hf, Al, or Pd (Table 3).

An additional, directly related error due to uncorrected secondary fluorescence in this system is the large overcorrection (for absorption) in the Pd measurement – the value is about 4 wt % too high – which accounts for the extremely high analytical total.

This study also demonstrates the potential problem with EDS software where analytical (elemental wt%) totals are normalized. Users would benefit if raw elemental totals were printed out, and the presence of high elemental totals could point to the possibility of the problem of secondary fluorescence.

CONCLUSION

EPMA is a powerful technique for precise compositional measurement of microvolumes. The generated X rays, however, have a 'life of their own' that differs fundamentally from the behavior of electrons used to initiate the process, and they can travel relatively far from the original target spot and create a secondary generation of X rays. These secondarily fluoresced X rays can be collected by the detector (both EDS and WDS) and yield erroneous measurement – both in elements of the secondary X rays, as well as in erroneous matrix corrections of the primary X-ray intensities.

We demonstrate here that the measurement of Nb $K\alpha$ X rays, utilizing high accelerating voltages (28–30 keV), yields significant errors both in the Nb and Pd concentrations of phases in an annealed eutectic assemblage. This is particularly exacerbated by the presence Pd $K\alpha$ X rays, whose energy is just above the Nb K edge, which are very efficient in exciting Nb $K\alpha$ X rays. This effect could be minimized by utilizing an accelerating voltage of 24 keV, whereby no Pd K X rays would be generated; however, there still would be some secondary fluorescence of Nb by the continuum X rays between 19 keV and the accelerating voltage value.

There are two solutions here: (i) utilizing only the Nb $L\alpha$ line, which we show has virtually no secondary fluorescence in more than $\sim 5 \mu\text{m}$ from the interface, or (ii) creating an accurate geometric model with PENELOPE, simulating the

secondary fluorescence at the analytical EPMA conditions, determining the correction factor, importing it into the EPMA software prior to matrix correction, and then calculating the matrix correction for the secondary-fluorescence-corrected *K*-ratio.

Acknowledgements

We thank John Donovan (University of Oregon) for development of Probe for Windows–Enterprise; David Snoeyenbos (CAMECA) for the LIF220 crystal holder and Edgar Chavez (CAMECA) for installation and alignment; Francesc Salvat and Xavier Llovet (Universitat de Barcelona) for generosity with their time and assistance with PENELOPE, as well as insights; and Dale Newbury, Cedric Powell and an anonymous reviewer for insightful comments.

REFERENCES

1. Reed SJB. *Electron Microprobe Analysis* (2nd edn). Cambridge University Press: Cambridge, 1993.
2. Donovan JJ, Fournelle JH. *Probe for Windows Reference Manual*: <http://epmalab.uoregon.edu/pfw/pfw-32.pdf>; 2005.
3. Armstrong JT. *Microsc. Microanal.* 1988; 239.
4. Drouin D, Couture A, Gauvin R. *Microsc. Microanal.* 2001; 7(2): 684.
5. Baro J, Sempau J, Fernandez-Varea JM, Salvat F. *Nucl. Instrum. Methods. Phys. Res., B* 1995; 100: 31.
6. Llovet X, Valovirta E, Heikinheim E. *Mikro. Acta* 2000; 132: 205.
7. Llovet X, Galan G. *Am. Mineral.* 2003; 88: 121.
8. Goldstein JI, Newbury DE, Echlin P, Joy DC, Romig Jr AD, Lyman CE, Fiori C, Lifshin E. *Scanning Electron Microscopy and X-ray Microanalysis* (2nd edn). Plenum Press: New York, 1992.